Characterization by Infrared Spectroscopy of the Interaction of a Cardiotoxin with Phosphatidic Acid and with Binary Mixtures of Phosphatidic Acid and Phosphatidylcholine†

André Désormeaux,‡ Gaétan Laroche,‡ Pierre E. Bougis,§ and Michel Pézolet*,‡

Centre de Recherche en Sciences et en Ingénierie des Macromolécules, Département de Chimie, Université Laval, Cité Universitaire, Québec G1K 7P4, Canada, and Laboratoire de Biochimie, Faculté de Médecine, Secteur Nord, Centre National de la Recherche Scientifique, Unité de Recherche Associée 1455, Boulevard Pierre Dramard, 13326 Marseille Cedex 15, France

Received July 27, 1992; Revised Manuscript Received September 23, 1992

ABSTRACT: The effect of cardiotoxin IIa from *Naja mossambica mossambica*, a small basic protein extracted from snake venom, on dimyristoylphosphatidic acid (DMPA) and on equimolar mixtures of DMPA and dimyristoylphosphatidylcholine (DMPC) has been studied by Fourier transform infrared spectroscopy. The interaction of cardiotoxin with DMPA dispersions decreases both the cooperativity of the phase transition of the lipid and the molecular order of the lipid acyl chains in the gel phase. This effect increases with the proportion of the toxin in the complexes and leads to the total abolition of the phase transition of DMPA at a lipid-to-protein molar ratio of 5. Small-angle X-ray results demonstrate that the structure of the lipid–protein complexes is poorly ordered and gives rise to broad diffusion peaks rather than to well-resolved diffraction patterns. Infrared spectra of oriented cardiotoxin–DMPA films show that the protein is not homogeneously oriented with respect to the bilayer surface. The destabilization of the gel-phase structure of DMPA by cardiotoxin also results in a deeper water penetration in the interfacial region of the lipid since more carbonyl ester groups appear to be hydrogen bonded in the presence of the toxin. The infrared results on the phosphate group vibrations also indicate clearly that the basic residues of cardiotoxin interact strongly with the phosphate group of DMPA that becomes partly ionized at a pH as low as 6.5. The results obtained on the interaction of cardiotoxin with an equimolar mixture of DMPA and DMPC clearly demonstrate the ability of this toxin to induce lateral phase separation in this mixture with one phase containing DMPA-rich domains perturbed by cardiotoxin while the second phase is composed of regions enriched in DMPC. Comparison of the results of the current study with those obtained on other basic proteins and polypeptides suggests that charge-induced phase separation occurs only when the charge density on certain regions of the protein structure is high enough to lead to efficient electrostatic interactions with anionic phospholipids. This condition occurs only when the conformation of the protein or polypeptide is well-ordered at the lipid interface.

Lateral phase separations in biological membranes are believed to be of primary importance in several physiological processes (Portis et al., 1979; Scheule, 1987). The occurrence of lateral phase separations leads to metastable defects and domains in membrane structure (Sackmann, 1983), with distinct physical properties and composition, that could result in specific transport mechanisms such as exocytosis and endocytosis (Poste & Allison, 1973; Papahadjopoulos et al., 1979). Moreover, because of the presence of such domains, proteins in the same membrane can be sequestered in unique environments, i.e., in separate microdomains where their activities may be optimized or modulated by specific lipid or protein interactions (Gennis, 1989).

Most charge-induced lateral phase separations observed until now were caused by divalent cations on binary mixtures of zwitterionic and negatively charged lipids (Onishi & Ito, 1974; Jacobson & Papahadjopoulos, 1975; Hui et al., 1983; Kouaouci et al., 1985; Graham et al., 1985). Only a few examples were reported on lateral phase separations induced by proteins or polypeptides. Boggs et al. (1977) have shown that myelin basic protein is able to induce partial phase separation in mixtures of dimyristoylphosphatidylglycerol (DMPG)[1] and dimyristoylphosphatidylcholine (DMPC). Laroche et al. (1988) have also reported that high molecular weight poly(L-lysine) (M_w = 180 000–260 000) induces partial phase separation in mixed lipid systems composed of dimyristoylphosphatidic acid (DMPA) and DMPC, while it has been shown that melittin also gives rise to peptide-enriched phases in mixtures of distearoylphosphatidylcholine (DSPC) and dipalmitoylphosphatidylglycerol (DPPG) (Lafleur et al., 1989).

Cardiotoxins are basic proteins extracted from snake venom. These toxins have a molecular weight of about 7000 and contain approximately 60 amino acid residues that are highly stabilized by the presence of four disulfide bridges. In vivo, cardiotoxins caused systolic cardiac arrest. However, there mechanism of action at the molecular level is still a matter of controversy, but there is a general agreement that car-

† This research was supported by research grants (M.P.), a postdoctoral fellowship (A.D.), and a scholarship (G.L.) from the Natural Sciences and Engineering Research Council of Canada and by the Fonds FCAR of the Province of Québec (M.P.). A.D. was also the recipient of a fellowship from the Fondation du Prêt d'Honneur du Québec.

* To whom correspondence should be addressed.

‡ Université Laval.

§ CNRS URA 1455.

[1] Abbreviations: ATR, attenuated total reflectance; CTX, cardiotoxin; DMPG, dimyristoylphosphatidylglycerol; DMPC, dimyristoylphosphatidylcholine; DMPA, dimyristoylphosphatidic acid; DSPC, distearoylphosphatidylcholine; DPPG, dipalmitoylphosphatidylglycerol; DMPC-d_{54}, DMPC with perdeuterated acyl chains; EDTA, ethylenediaminetetraacetic acid; R_i, phospholipid-to-protein molar ratio; NMR, nuclear magnetic resonance; PC, phosphatidylcholine; PA, phosphatidic acid; PG, phosphatidylglycerol; PLL, poly(L-lysine).

0006-2960/92/0431-12173$03.00/0

diotoxins act by perturbing the lipid phase of cell membranes (Bougis et al., 1983; Ménez et al., 1990). The three-dimensional structure of cardiotoxins has been recently determined by X-ray crystallography (Rees et al., 1987) and NMR spectroscopy (Steinmetz et al., 1988). Both studies show that cardiotoxins consist mainly of three hairpin loops forming an oblate ellipsoid in which the peptide chain forms a double-stranded and a triple-stranded antiparallel β-sheet. The topology of cardiotoxins is, therefore, very similar to that found in short and long snake neurotoxins, which block the nicotinic acetylcholine receptor. The high content of β-sheet conformation in cardiotoxins has also been revealed from the determination of the secondary structure of the protein by circular dichroism (Visser & Louw, 1978; Ménez et al., 1978), Raman spectroscopy (Pézolet et al., 1982), and infrared spectroscopy (Surewicz et al., 1988).

Cardiotoxins are known to interact only with negatively charged lipids (Dufourcq & Faucon, 1978; Vincent et al., 1978). The interaction of cardiotoxins with DMPA bilayers leads to only a small perturbation of their conformation (Pézolet et al., 1982), while their binding to DMPG results in an increase of the content of the β-structure at the expense of the unordered conformation (Surewicz et al., 1988). Furthermore, results obtained on phospholipid monolayers (Bougis et al., 1981) and by Raman (Faucon et al., 1983) and fluorescence spectroscopies (Dufourcq & Faucon, 1978; Vincent et al., 1978) suggest that the initial electrostatic interaction of cardiotoxins at the bilayer surface is followed by the penetration of one hydrophobic loop into the bilayer core. This leads to hydrophobic interactions between some apolar residues of cardiotoxins and the acyl chains of the phospholipid bilayers. Finally, fluorescence measurements have shown that each cardiotoxin molecule can bind up to seven phospholipid molecules when the lipid head group bears only one negative charge or 3.5 when the lipid is doubly ionized (Dufourcq & Faucon, 1978; Faucon et al., 1983).

Even though the effect of cardiotoxins on the structure of the acyl chain region of negatively charged phospholipids has been investigated by several methods, no data are available on the effect of these proteins on the interfacial and polar head group regions of phospholipids. Infrared spectroscopy has thus been used in this report to investigate the effect of cardiotoxin IIa from *Naja mossambica mossambica* on the conformation and orientation of the acyl chains and interfacial and polar head regions of aqueous dispersions of DMPA. Furthermore, it was verified if charge-induced phase separation can arise when this cardiotoxin interacts with a binary mixture of phospholipids composed of DMPA and DMPC. To answer this question, vibrational spectroscopy is particularly effective since perdeuteration of the acyl chains of one lipid component of the mixture allows the simultaneous and independent determination of the conformational properties of both lipids in the mixture (Mendelsohn & Tarashi, 1978; Mendelsohn & Maisano, 1978; Laroche et al., 1988; Lafleur et al., 1989; Devlin & Levin, 1989).

MATERIALS AND METHODS

Materials. The disodium salt of dimyristoylphosphatidic acid (DMPA) and dimyristoylphosphatidylcholine with perdeuterated acyl chains (DMPC-d_{54}) were obtained from Avanti Polar Lipids (Birmingham, AL) and used without further purification. Cardiotoxin IIa, hereafter called cardiotoxin, was purified from *N. m. mossambica* venom according to the method described by Bougis et al. (1986).

Sample Preparation. Solutions of cardiotoxin were prepared in 150 mM NaCl and 10 mM EDTA at a protein concentration of either 7% by weight for the measurement of the infrared spectra or 2% for the preparation of the lipid–protein complexes. The pH of the solutions was measured with a microelectrode (Microelectrodes, Inc., Londonderry, NH) and adjusted to pH 6.5 with diluted NaOH or HCl solutions. Binary phospholipid mixtures were prepared by dissolving appropriate amounts of each component in chloroform/methanol (87:3 v/v). After complete dissolution of the solid, the solvent was evaporated under a stream of nitrogen, and final traces of solvent were removed by pumping overnight over the sample in a vacuum desiccator.

Aqueous dispersions of DMPA, DMPC-d_{54}, and mixtures of these lipids were prepared by mixing appropriate amounts of solids in a solution containing 150 mM NaCl and 10 mM EDTA, adjusted to pH 6.5 with diluted NaOH or HCl solutions. Samples containing about 7% by weight in total lipids were then heated to approximately 65 °C for 10 min, stirred on a vortex mixer, and cooled down below the gel-to-liquid crystalline phase transition temperature. This cycle was repeated at least three times. The pH of the dispersions was adjusted to pH 6.5, if necessary. Lipid dispersions used to make lipid-protein complexes were prepared similarly except that the lipid concentration was 1%. Lipid–protein complexes were prepared by adding appropriate amounts of a 2% cardiotoxin solution to phospholipid dispersions in order to obtain the desired DMPA-to-protein molar ratio (R_i). The incubation cycle was then repeated once again and the resulting samples were centrifuged to yield white pellets that were used for infrared and X-ray experiments.

Infrared Experiments. Protein solutions or lipid–protein pellets were transferred in an infrared transmission cell composed of two BaF_2 windows separated with 6- or 10-μm Teflon spacers, respectively (Dousseau et al., 1989). The infrared cell was placed in a thermoelectrically regulated sample holder as described elsewhere (Pézolet et al., 1983). Spectra were recorded with a Bomem, Hartmann and Braun (Québec, Canada) DA3-02 Fourier transform infrared spectrometer with a narrow-band mercury–cadmium–telluride detector and a germanium-coated KBr beamsplitter. A total of 1000 scans for the protein solutions and 250 scans for the lipid–protein complexes were routinely taken with a maximal optical retardation of 0.5 cm, coadded, triangularly apodized, and Fourier transformed to yield a resolution of 2 cm^{-1}.

Oriented multilayers of DMPA and DMPA–cardiotoxin complexes (R_i = 20) were obtained by slowly spreading aqueous samples with a Teflon bar on one side of germanium attenuated total reflectance (ATR) plates (50- × 10- × 2-mm 45° parallelograms) until dry films were obtained. Prior to the sample deposition, the ATR plates were cleaned with a plasma cleaner (Harrick Scientific, Ossining, NY) in order to make the surface more hydrophilic. The plates on which the dry films were supported were placed in a variable-angle ATR unit (Harrick, NY) preceded by a rotating wire-grid polarizer (Specac, Orpington, U.K.). A total of 500 scans were coadded for each polarization at a resolution of 2 cm^{-1}. The efficiency of the deposition was checked by measuring the dichroic ratio of the CH_2 wagging band progression between 1200 and 1300 cm^{-1}.

Dichroic ratios (R) of the infrared bands were obtained by determining the ratio of either the peak heights or the integrated intensities of the bands measured with the incident light polarized parallel and perpendicular with respect to the plane of incidence ($A_\parallel/A_\perp$) (Fringeli & Günthard, 1981). Assuming a uniaxial fiber-type distribution of orientation with respect to the normal to the ATR crystal, the order parameters $f(\theta)$, relating the orientation of the fiber axis and the normal

to the ATR crystal, were calculated using the following formula (Hübner & Mantsch, 1991):

$$f(\theta) = \frac{R-2}{R+1.45}\,\frac{2}{3\cos^2\gamma - 1}$$

where γ is the angle between the transition moment of a given vibration and the fiber axis. The angle γ was set to 0° for the protein amide vibrations as well as for the vibrations of the lipid head group and CH_2 wagging band progression, while it was set to 90° for the acyl chain CH_2 stretching and bending vibrations. The mean angle θ between the fiber axis and the normal to the ATR crystal was then calculated from

$$f(\theta) = \frac{3\cos^2\theta - 1}{2}$$

All data manipulations were performed with Spectra Calc software (Galactic Industries Corp.). The position of the infrared bands was calculated from the frequency of the center of gravity of 90% of the height of the bands due to the CH_2 and CD_2 symmetric stretching modes. The estimation of the secondary structure of cardiotoxin in aqueous solution from its infrared spectrum was obtained by the method developed by Dousseau and Pézolet (1990).

Small-Angle X-Ray Experiments. Samples were transferred into X-ray thin-wall glass capillary tubes of 1.0-mm diameter which were centrifuged and sealed. Measurements were performed on a Rigaku/Rotaflex rotating anode generator (Model RU-200 BH), operated at 55 kV and 190 mA, using the nickel-filtered Cu Kα line (λ = 1.5418 Å). The beam was focused by two pinholes of 0.20- and 0.15-mm diameter. Diffraction patterns were recorded at room temperature with a scan rate of 0.01°/min using a scintillation counter.

RESULTS

Interaction of Cardiotoxin with Pure DMPA Dispersions. For the study of the conformational properties and thermotropic behavior of phospholipids, the infrared bands appearing in the C–H stretching mode region (2700–3100 cm^{-1}) are particularly well suited since they are sensitive to the conformation and the dynamics of the phospholipid acyl chains (Snyder et al., 1978; Umemura et al., 1980). Figure 1 shows the C–H stretching mode region of the infrared spectrum of a pure DMPA dispersion below and above the temperature of the gel-to-fluid phase transition of the lipid. This spectral region is dominated by two strong bands at 2917 and 2850 cm^{-1} due to the methylene antisymmetric and symmetric stretching modes, respectively. Weaker bands due to the asymmetric and symmetric stretching modes of the terminal methyl groups are also present at 2956 and 2872 cm^{-1}, respectively. One can observed that the gel-to-fluid phase transition of DMPA is accompanied by a simultaneous broadening and shift toward higher frequencies of the 2850- and 2917-cm^{-1} features. Earlier studies have assigned the broadening of these bands to the increase of the rotational mobility of the acyl chains and their frequency shift to the introduction of gauche conformers along the lipid acyl chains (Umemura et al., 1980). The effect of cardiotoxin on the infrared spectrum of DMPA in the gel and fluid phases is also shown in Figure 1. In the gel phase, it is clear that cardiotoxin induces an important disordering of the lipid acyl chains since the 2850- and 2917-cm^{-1} features are broader and appear at higher frequency in the presence of the toxin. In the fluid phase, the spectral perturbation induced by cardiotoxin is much less pronounced.

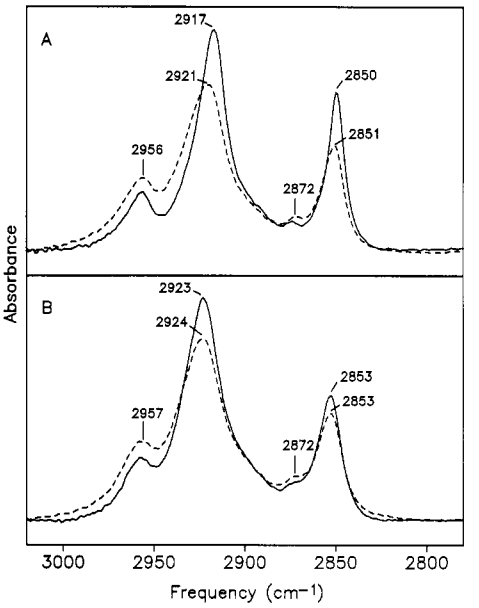

FIGURE 1: Infrared spectra in the C–H stretching mode region of DMPA (—) and of DMPA–cardiotoxin complexes at R_i = 10 (- - -) in the (A) gel (20 °C) and (B) liquid crystalline (70 °C) phases.

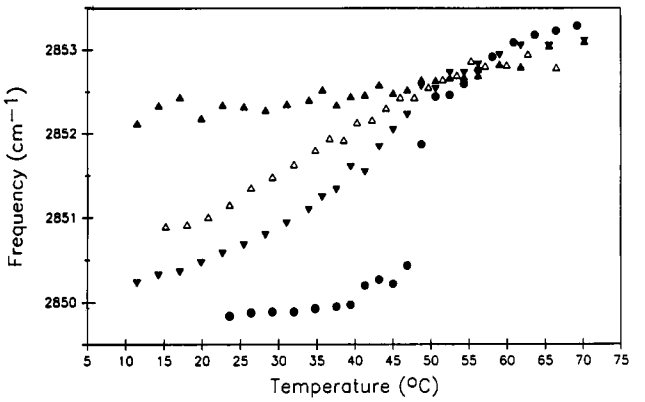

FIGURE 2: Temperature profiles of DMPA derived from the frequency of the infrared methylene stretching mode in the absence (●) and in the presence of cardiotoxin at R_i = 15 (▼), R_i = 10 (△), and R_i = 5 (▲).

Figure 2 shows the temperature dependence of the frequency of the 2850-cm^{-1} band for DMPA dispersions in the absence and presence of cardiotoxin at various lipid-to-protein molar ratios. The 2850-cm^{-1} feature was used instead of the 2917-cm^{-1} band since it is less affected by the spectral contribution of the protein. As seen in this figure, there is a major shift of the 2850-cm^{-1} band in the infrared spectrum of DMPA dispersion at about 49 °C, as the lipid undergoes the gel-to-fluid phase transition. This result is in good agreement with previous data obtained by differential scanning calorimetry (Van Dijck et al., 1978; Graham et al., 1985), Raman spectroscopy (Mushayakarara & Levin, 1984; Laroche et al., 1988), and ^{2}H-NMR spectroscopy (Laroche et al., 1990). In the presence of cardiotoxin, there is an increase of the frequency of the 2850-cm^{-1} feature in the gel phase, indicating that the interaction of the protein with DMPA leads to the introduction of gauche conformers in the lipid acyl chains. Moreover, this effect is more pronounced as the lipid-to-protein molar ratio decreases. On the other hand, the toxin has almost no effect on the frequency of the 2850-cm^{-1} feature in the fluid phase so that the gel-to-fluid phase transition of the lipid is much less cooperative and occurs at slightly lower temperatures as the lipid-to-protein molar ratio decreases. Fur-

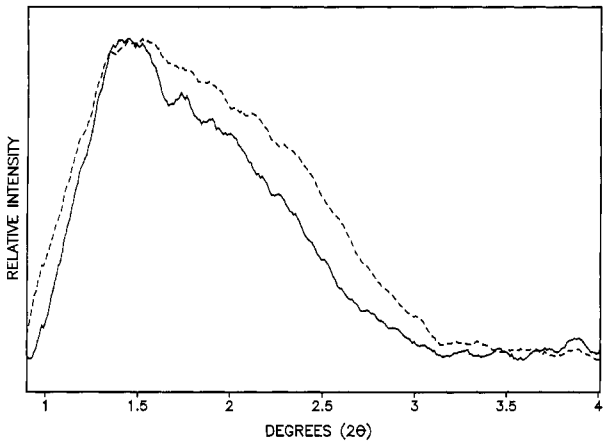

FIGURE 3: Small-angle X-ray diffraction patterns of DMPA–cardiotoxin complexes at R_i = 15 (—) and R_i = 5 (- - -).

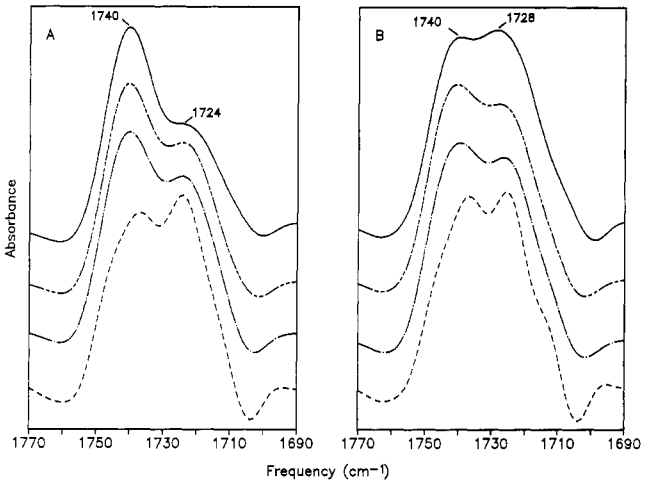

FIGURE 4: Fourier deconvolved infrared spectra of the carbonyl stretching mode region of DMPA (—) and DMPA–cardiotoxin complexes at R_i = 15 (– – –), R_i = 10 (– · –), and R_i = 5 (- - -) in the (A) gel (20 °C) and (B) liquid crystalline (70 °C) phases. Deconvolution was made according to the method of Griffiths and Pariente (1986) using a deconvolution parameter γ of 2.2 and an apodization filter of 0.22.

thermore, the transition becomes totally abolished at a lipid-to-protein molar ratio of 5.

In order to investigate the type of structure adopted by the DMPA–cardiotoxin complexes, small-angle X-ray experiments were performed on complexes with various lipid-to-protein molar ratios. As opposed to X-ray experiments on the DMPA–Ca^{2+} system, where the well-ordered lamellar phase produces several diffraction orders (Liao & Prestegard, 1981; Laroche et al., 1991), DMPA–cardiotoxin complexes give rise to broad diffusion patterns (Figure 3). This could be due either to the presence of lamellar structures with variable repeat distance between the lamellae or to the coexistence of several structures such as the lamellar, micellar, vesicular, or hexagonal phases. For the latter case, the predominant phase is not the hexagonal one since the observed pattern is not typical of this structure (Shyamsunder et al., 1988).

The effect of cardiotoxin on the interfacial and polar head group regions of DMPA has also been studied from the carbonyl and phosphate stretching mode regions of the infrared spectra. Figure 4 displays the carbonyl stretching mode region of the deconvolved infrared spectra of DMPA dispersions in the absence and in the presence of cardiotoxin below and above the gel-to-fluid phase transition temperature of the lipid. As can be seen on the spectrum of the pure lipid in the gel phase, two components are present at 1740 and 1724 cm^{-1}.

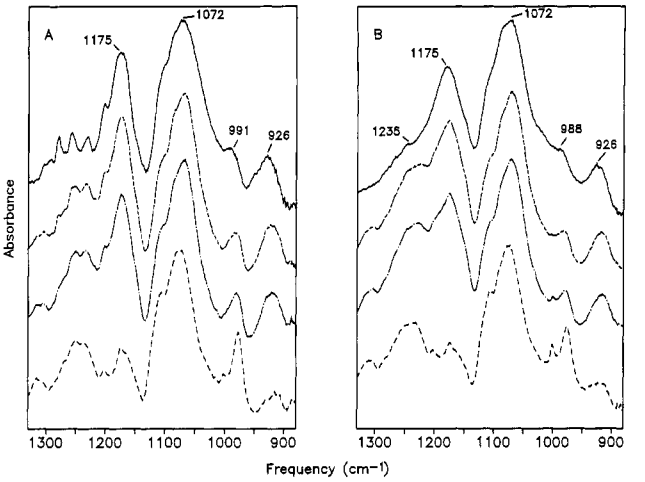

FIGURE 5: Infrared spectra of the phosphate stretching mode region of DMPA (—) and DMPA–cardiotoxin complexes at R_i = 15 (– – –), R_i = 10 (– · –), and R_i = 5 (- - -) in the (A) gel (15 °C) and (B) liquid crystalline (70 °C) phases.

Blume et al. (1988), have shown that the low-frequency component is mainly due to phospholipid carbonyl groups that are hydrogen-bonded to water, while the high-frequency feature is assigned to non-hydrogen-bonded C=O groups. This spectral region was shown to be particularly effective to characterize the hydration of the carbonyl groups in DMPA–Ca^{2+} complexes (Laroche et al., 1991).

For pure DMPA in the gel phase (Figure 4), the value of the peak height intensity ratio of the 1740-cm^{-1} component with respect to the 1724-cm^{-1} feature, h_{1740}/h_{1724}, is 1.87, showing that slightly less than half of the carbonyl groups are hydrogen-bonded to water molecules for this lipid, in good agreement with the infrared results of Blume et al. (1988). A similar effect has also been observed with DMPG (Blume et al., 1988) and DPPG bilayers (Babin et al., 1987). On the other hand, in the spectrum of DMPA in the fluid phase, both features of the carbonyl band have almost equal intensity (h_{1740}/h_{1724} = 0.97), revealing that more carbonyl groups are hydrogen-bonded than in the gel phase.

The addition of cardiotoxin to DMPA bilayers induces important modifications of the carbonyl stretching mode region (Figure 4). In the gel phase, the h_{1740}/h_{1724} ratio decreases with the increase of the protein content, indicating that more carbonyl groups are hydrated in the presence of the protein, and reaches a value of 0.90 for the R_i = 5 complexes. In fact, since the toxin has almost no effect on the ester carbonyl spectrum of DMPA in the liquid crystalline phase, at R_i = 5, the h_{1740}/h_{1724} ratio is almost identical for both the gel and the liquid crystalline phases of the lipid. This result is in agreement with the temperature dependence of the 2850-cm^{-1} methylene band (Figure 2) showing that for the R_i = 5 complex no thermotropic transition is observed.

The phosphate stretching mode region of the infrared spectra of phospholipid systems is also very useful to monitor the effect of the binding of positively charged species on the lipid head group (Dluhy et al., 1983; Casal et al., 1987a,b; Laroche et al., 1991). Figure 5 shows this spectral region for pure DMPA bilayers and for DMPA–cardiotoxin complexes. The 1175-cm^{-1} band in the infrared spectra of pure DMPA is due to the PO_2^- antisymmetric stretching mode while the band observed at 1072 cm^{-1} is assigned to the PO_2^- symmetric stretching mode (Shimanouchi et al., 1964; Thomas & Chittenden, 1970; Casal et al., 1987a,b). The weak bands superimposed with the PO_2^- antisymmetric stretching component in the gel phase are due to the acyl chains methylene

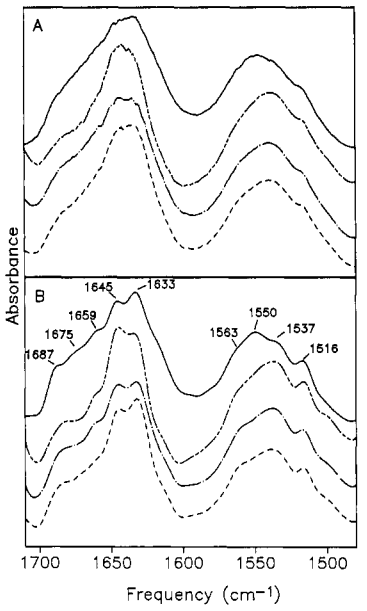

FIGURE 6: Infrared spectra at 20 °C of the amide I and amide II regions of cardiotoxin in the absence (—) and in the presence of aqueous dispersions of DMPA at R_i = 15 (– – –), R_i = 10 (– · –), and R_i = 5 (- - -). (A) Original and (B) Fourier deconvolved spectra. Deconvolution was made according to the method of Griffiths and Pariente (1986) using a deconvolution parameter γ of 2.2 and an apodization filter of 0.22.

wagging progression (Casal & Mantsch, 1984) and are characteristic of lipid acyl chains in an all-trans conformation. Features characteristic of the P–O–(C) and P–O–(H) stretching modes are observed at 991 and 926 cm^{-1}, respectively (Thomas & Chittenden, 1964). Finally, the broad band observed around 1235 cm^{-1} for the DMPA–cardiotoxin complexes is due to the amide III band of the protein.

As seen in Figure 5, at both low and high temperatures, the bands due to the phosphate vibrations are more and more affected as the proportion of cardiotoxin increases. Compared to the pure lipid, at R_i = 5 the intensity of the 1175-cm^{-1} band is much weaker while a new band is observed at 977 cm^{-1}. This spectral change indicates clearly that the interaction of cardiotoxin with DMPA results, at least partly, in the ionization of the second OH group of the lipid at pH 6.5. The presence of the additional charge on the lipid head group gives rise to a distinct infrared spectrum due to the change of the symmetry of the phosphate group, which is isomorphic with the C_{3v} point group. For example, the infrared bands due to the symmetric and antisymmetric PO_3^{2-} stretching modes were observed around 985 and 1100 cm^{-1}, respectively, for doubly ionized dihexadecylphosphatidic acid (Laroche et al., 1991) and monomethyl phosphate (Hauser et al., 1990). The ionization of the second OH group of DMPA is further supported by the gradual decrease of the intensity of the 926-cm^{-1} band, associated with the P–O–(H) stretching mode, with the increase of the proportion of cardiotoxin in the complexes.

The conformation of cardiotoxin has also been investigated from the amide I and amide II spectral region. Figure 6A shows the infrared spectrum of an aqueous solution of the protein (pH 6.5) after correction for the spectral contribution of the water bending vibration according to the method of Dousseau et al. (1989). Figure 6A shows that the amide I and amide II bands of the protein are centered at 1637 and 1548 cm^{-1}, respectively, indicating that the toxin is mainly composed of β-sheet structure. Additional information on the conformation of the toxin can be obtained from the Fourier deconvolved spectrum of the protein (Figure 6B). As seen in this figure, in addition to the characteristic absorption frequency of the β-sheet conformation at 1633 cm^{-1}, weaker components are observed at 1687, 1675, 1659, and 1645 cm^{-1}. The 1659- and 1645-cm^{-1} bands can be assigned easily to α-helix and unordered structures, respectively (Byler & Susi, 1986; Surewicz & Mantsch, 1988; Surewicz et al., 1990; Muga et al, 1990). The assignment of the 1675- and 1687-cm^{-1} bands is less clear; they have been alternatively associated with the high-frequency component of the amide I vibration of the β-sheet conformation (Byler & Susi, 1986) or with β-turns (Dong et al., 1990). Recent results on wheat ω-gliadins, which are gluten proteins with a high content of β-turns, have shown that this type of conformation absorbs predominantly around 1675 cm^{-1} (Pézolet et al., 1992). We, therefore, assigned the 1675-cm^{-1} component to the presence of β-turns in cardiotoxin. The results obtained from the method of Dousseau and Pézolet (1990) reveal that the secondary structure content of cardiotoxin is 56% ± 4% β-sheets, 41% ± 5% unordered or β-turns, and only 3% ± 5% α-helical. This secondary structure is quantitatively in excellent agreement with the 50% β-sheet content obtained from the three-dimensional structure determined by NMR spectroscopy in solution (Steinmetz et al., 1988).

The infrared spectrum of cardiotoxin in the presence of DMPA has also been investigated in order to probe for lipid-induced conformational changes. Since the water spectrum is affected by the presence of lipids, the infrared spectra of the DMPA–cardiotoxin complexes cannot be adequately corrected for the water contribution, and consequently, only qualitative results can be obtained about the conformation of the toxin in the complexes. The deconvolved spectra (Figure 6B) show that, in the presence of the lipid, the amide I band is significantly narrower, suggesting that the β-sheet structure is more uniform, in agreement with previous Raman results (Pézolet et al., 1982). In particular, the intensity of the high-frequency shoulders due to β-turns (1675 cm^{-1}) and α-helices (1659 cm^{-1}) is reduced in the spectra of DMPA-cardiotoxin complexes. Figure 6 also reveals that there is a marked increase of the intensity of the 1537-cm^{-1} amide II band in the presence of cardiotoxin. Although the amide II spectral region has not been widely investigated in the literature, the 1537-cm^{-1} band has been assigned to antiparallel β-sheets (Krimm & Bandekar, 1986). Therefore, both the amide I and amide II regions indicate that the interaction of cardiotoxin with DMPA results in a stabilization of the antiparallel β-sheet structure of the protein. Spectra in the amide I and amide II regions also show that the structure of the protein is very stable up to at least 70 °C.

In order to get deeper insight into the molecular organization of the complexes formed by cardiotoxin and DMPA, polarized infrared ATR spectra of oriented films of pure DMPA and of a DMPA–cardiotoxin complex (R_i = 20) were recorded. Figure 7 shows the spectra obtained for the lipid–protein complex with the incident light polarized parallel and perpendicular to the plane of incidence as well as the difference spectrum. These spectra show clearly that the lipid molecules are highly oriented in the film since the series of bands in the 1200–1300-cm^{-1} region due to the CH_2 wagging band progression (transition moment along the direction of the all-trans methylene chains) are strongly polarized. The assignments of the most relevant infrared bands are listed in Table I together with their dichroic ratio, the calculated order parameters, and the mean angles θ.

From Table I, the average value of the order parameter for the bands due to the all-trans acyl chains in the film of pure

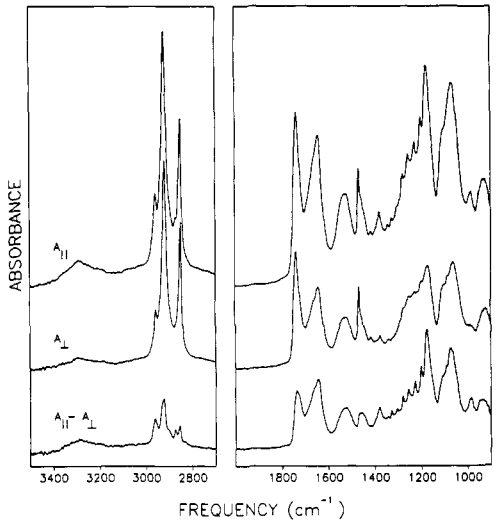

FIGURE 7: Polarized ATR infrared spectra of an oriented DMPA–cardiotoxin film (R_i = 20) measured with the polarization of the incident light parallel ($A_{\parallel}$) and perpendicular ($A_{\perp}$) to plane of incidence. The difference between the two spectra ($A_{\parallel} - A_{\perp}$) is shown at the bottom of the figure.

DMPA (1203, 1229, 1467, 2851, and 2920 cm^{-1}) is 0.74, showing that the acyl chains of the lipids are tilted with an angle of 25° with respect to the normal to the ATR crystal. This is in excellent agreement with the tilt angle of 24° observed in the crystal structure of DMPA (Harlos et al., 1984) and suggests that the bilayers are well-ordered and lie flat on the surface of the crystal. In the presence of the protein the average value of the order parameter for the different CH_2 modes decreases to 0.58. This change could be due either to the further increase of the chain tilt angle by the protein or, as seen above from frequency of the CH_2 modes, to the introduction by cardiotoxin of gauche conformers along the all-trans methylene chains which change the angle γ between the transition moments and the chain axis. For pure DMPA, the ester C = O groups of the lipid are on average oriented at 64° relative to the bilayer plane, as has also been observed for phosphatidylcholines (Hübner & Mantsch, 1991). As seen in Table I, the presence of the protein does not seem to affect the carbonyl orientation. The order parameters calculated for the symmetric and antisymmetric stretching vibrations of the PO_2^- group and for the stretching of the P–O–(H) bond are close to 0 whether the protein is present or not. This result suggests that the transition moments for these vibrations are randomly oriented and the phosphate groups are free to rotate around the phosphoester linkage.

The order parameter calculated for the amide I band of cardiotoxin bound to DMPA is also very close to 0. This leads to the conclusion that the transition moment for the amide I vibration, which lies in the peptide plane and is oriented at 15° from the C = O bond direction (Rothschild & Clark, 1979), either is oriented at 54.7° (the so-called magic angle) from the bilayer normal or is randomly oriented. Since the order parameters calculated for both the amide A and amide II are also close to 0, it is more likely that the amide bonds of cardiotoxin bound to DMPA are randomly oriented. In addition, order parameters calculated for the individual components of the amide I band after deconvolution and band fitting (results not shown) were all very close to 0.

Interaction of Cardiotoxin with a 1:1 DMPA–DMPC-d_{54} Mixture. In order to characterize the effect of cardiotoxin on DMPA–DMPC-d_{54} mixtures, infrared spectroscopy is particularly useful since the use of DMPC with perdeuterated acyl chains allows the independent determination of the thermotropic behavior of DMPA and DMPC in the mixture. DMPA was followed from the frequency of the CH_2 symmetric stretching model near 2850 cm^{-1}, while the frequency of the CD_2 symmetric stretching mode near 2090 cm^{-1} (Sunder et al., 1978) was used to follow the zwitterionic component of the mixture. It has been shown that the frequency of these bands monitors mainly the introduction of gauche conformers along the lipid acyl chains (Asher & Levin, 1977; Cameron et al., 1980).

Figure 8 displays the temperature profiles of each lipid component in aqueous dispersions of an equimolar mixture of DMPA and DMPC-d_{54} in the absence and in the presence of cardiotoxin at various lipid-to-protein molar ratios. As observed previously (Kouaouci et al., 1985; Laroche et al., 1988; Graham et al., 1985), these two lipids are miscible at equimolar concentration since only one transition with a midpoint temperature of about 38 °C is observed on the temperature profile derived from either the PC or the PA component. In addition, the two curves plotted with the same amplitude are perfectly superimposable (results not shown). The addition of cardiotoxin to the mixture affects strongly the temperature profile of the DMPA transition (Figure 8A). As observed in the case of DMPA–cardiotoxin complexes (Figure 2), when the proportion of the toxin increases, the gel-to-fluid phase transition of DMPA in the mixture shifts toward lower temperatures and becomes less cooperative due to an important decrease of the molecular order in the gel phase. In fact, at R_i = 5 with respect to the anionic lipid, the thermotropic behavior of DMPA in the mixture is very similar to that of DMPA alone in the presence of cardiotoxin (Figure 2).

The effect of cardiotoxin on the thermotropic behavior of the zwitterionic component (Figure 8B) of the equimolar mixture is quite different from that of the anionic component. The addition of the toxin to the binary mixture also shifts the phase transition of DMPC-d_{54} toward lower temperatures but the temperature profiles remain cooperative even at high proportions of cardiotoxin. The conformational order of the deuterated lipid in the gel phase, as revealed by the frequency of the 2090-cm^{-1} band, is only slightly affected by the presence of the protein. At R_i = 5, the transition observed for DMPC-d_{54} in the mixture is centered at about 25 °C, which is quite close to the transition of pure DMPC-d_{54} (18 °C). These results unambiguously indicate that the DMPA component in the equimolar mixture is more perturbed by cardiotoxin and that a phase richer in DMPC-d_{54} is formed.

DISCUSSION

The results obtained by infrared spectroscopy show that the interaction of cardiotoxin with DMPA leads to a marked decrease of the conformational order of the phospholipid acyl chains below the normal gel-to-fluid phase transition temperature of DMPA, while no toxin-induced conformational change of the lipid acyl chains is detected by infrared spectroscopy in the fluid phase. This leads to a gradual decrease of the cooperativity of the gel-to-fluid phase transition of the lipid as the proportion of the toxin in the complexes increases. The transition of DMPA is totally abolished at a lipid-to-protein molar ratio of 5, in agreement with the stoichiometry of the lipid–cardiotoxin complexes obtained from measurements of the intrinsic fluorescence of the tryptophan residue of cardiotoxin bound to negatively charged phospholipids (Dufourcq & Faucon, 1978; Faucon et al., 1983). The perturbation by cardiotoxin of the acyl chain conformation of DMPA below the gel-to-fluid phase transition temperature

Table I: Dichroic Ratio R, Order Parameter $f(\theta)$, and Calculated Angle θ for Selected Absorption Bands of DMPA and DMPA–Cardiotoxin Films

		DMPA[a]			DMPA–CTX, R_i = 20		
assignment	frequency (cm^{-1})	R	$f(\theta)$	θ	R	$f(\theta)$	θ
amide A	3295				1.96	–0.01	*b*
νCH_2 antisym	2920	1.02	0.80	21	1.14	0.66	*c*
νCH_2 sym	2851	1.09	0.72	26	1.20	0.60	*c*
$\nu C{=}O$	1737	1.40	–0.21	64	1.47	–0.18	62
amide I	1639				1.88	–0.03	*b*
amide II	1529				1.80	–0.06	*b*
δCH_2	1467	1.09	0.72	26	1.26	0.54	*c*
CH_2 wagging	1229	17.0	0.81	21	6.50	0.57	*c*
CH_2 wagging	1203	8.20	0.64	29	6.15	0.54	*c*
νPO_2^- antisym	1173	2.36	0.09	*b*	2.19	0.05	*b*
νPO_2^- sym	1064	2.06	0.02	*b*	1.98	–0.01	*b*
νP–O–(C)	986	6.56	0.57	32	5.07	0.47	36
νP–O–(H)	923	1.79	–0.07	*b*	1.92	–0.02	*b*

[a] The order parameter $f(\theta)$ and the angle θ for the methylene vibrations were calculated for all-trans hydrocarbon chains (see Materials and Methods). [b] Probably near random orientation. [c] The angle θ between the chain axis and the bilayer normal was not calculated for these vibrations because of the presence of gauche conformers due to the protein binding.

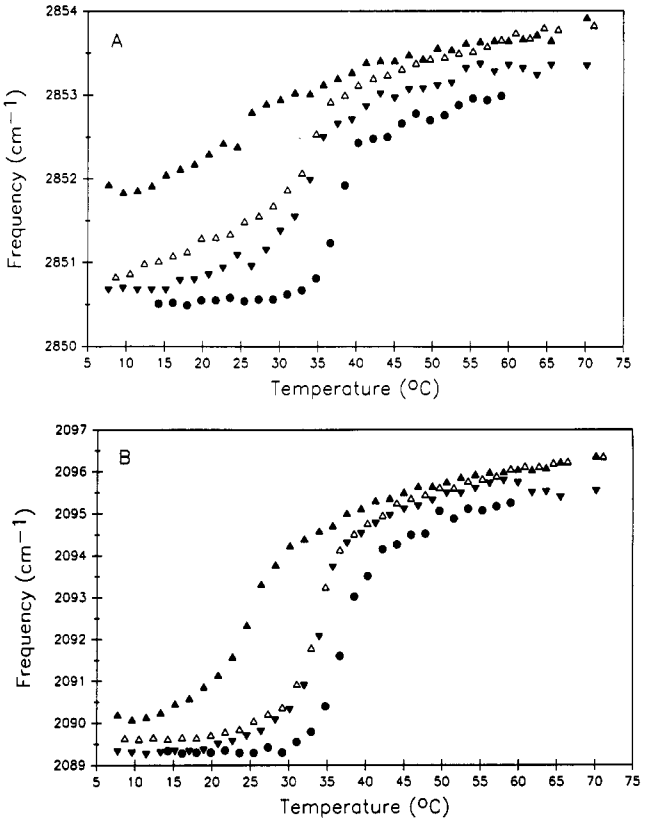

FIGURE 8: Temperature profiles of (A) DMPA and (B) DMPC-d_{54} derived from the frequency of the infrared CH_2 and CD_2 stretching modes, respectively, for an equimolar mixture of DMPA and DMPC-d_{54} in the absence (●) and in the presence of cardiotoxin at R_i = 15 (▼), R_i = 10 (△), and R_i = 5 (▲). The lipid-to-protein molar ratios are with respect to DMPA only.

suggests that the toxin destabilizes considerably the bilayer structure of DMPA as observed previously by other physical techniques (Faucon et al, 1983). This is further supported by the decrease of the order parameter of the lipid acyl chains (Table I) and by the broad diffraction patterns observed by small-angle X-ray scattering for the DMPA–cardiotoxin complexes.

The results obtained from the phosphate stretching mode region of the infrared spectrum of DMPA clearly demonstrate that the electrostatic interaction between the basic residues of the toxin and the phosphate group of the lipid is quite strong and leads to the gradual replacement of the second ionizable proton of the lipid at pH as low as 6.5. Although such an effect has already been observed for DMPA–Ca^{2+} complexes (Laroche et al., 1991), it was not encountered for the binding of polylysine to the same lipid (G. Laroche & M. Pézolet, unpublished). These infrared results prove unambiguously the assumption of Dufourcq and Faucon (1978), based on fluorescence measurements, that the binding of cardiotoxin to DMPA bilayers causes the ionization of the second acidic group of the lipid at pH 6.5, even though its pK_a should be between 8 and 9 (Traüble & Eibl, 1974; Galla & Sackmann, 1975).

The binding of cardiotoxin to DMPA has also a marked effect on the interfacial region of the lipid. For instance, below the normal phase transition temperature of DMPA, the toxin induces a large increase of the intensity of the low-frequency component of the carbonyl band as the proportion of the protein in the complexes increases, indicating an increase of the number of carbonyl groups that are hydrogen-bonded to water molecules. Therefore, in the presence of cardiotoxin, it seems that water molecules penetrate more deeply toward the glycerol backbone of DMPA. Such perturbations of the interfacial region of charged phospholipids might be at the origin of the synergetic increase of the phospholipase A_2 activity observed in natural membranes (Rivas et al., 1981) in the presence of cardiotoxin.

The infrared results on the conformation-sensitive amide I and amide II regions show that the interaction of cardiotoxin with DMPA bilayers does not lead to a major reorganization of the protein structure. As shown previously by Raman spectroscopy (Pézolet et al., 1982), the four disulfide bridges are not affected by the binding of the toxin to DMPA bilayers. The tight tertiary structure of cardiotoxin is thus preserved, even in the presence of the charged lipid. Nevertheless, the infrared spectra of the protein bound to DMPA show a decrease of the bandwidth of the amide I band and an increase of the intensity of the 1537-cm^{-1} feature assigned to the amide II vibration of the antiparallel β-sheet structure, compared to the lipid-free protein. Therefore, the interaction of cardiotoxin with DMPA stabilizes the antiparallel β-sheet structure of the protein and also results in the decrease of the number of turns. Since most of the positively charged residues of cardiotoxin are located in the central part of the molecule where the triple-stranded antiparallel β-sheet structure is observed (Steinmetz et al., 1988), it is likely that the conformational change detected by infrared spectroscopy results from the neutralization of the charge of these residues

by the phosphate group of DMPA molecules.

Three models have been proposed for the interaction between cardiotoxins and acidic phospholipids. According to Lauterwein and Wüthrich (1978), all three hydrophobic loops of cardiotoxin are embedded in the hydrophobic core of the membrane. The central loop crosses completely the bilayer, exposing the charged residues on its tip for interaction with the lipid phosphate groups at the opposite side of the bilayer. Dufourcq et al. (1982) have proposed that the initial electrostatic interaction of the basic residues of cardiotoxins with negatively charged phospholipids is followed by the penetration of at least the N-terminal hydrophobic loop into the bilayer. Finally, Batenburg et al. (1985) have suggested that, in the case of the interaction of cardiotoxin with cardiolipin, the protein resides with its polar part in the interior of two inverted micelles and its hydrophobic β-pleated sheet in the acyl chain region.

The model of Lauterwin and Wüthrich (1978) accounts for the high affinity and the stoichiometry of the binding of cardiotoxin and negatively charged phospholipids. However, the charged residues of the tip of the central loop have to cross the hydrophobic core of the bilayers to interact with the phosphate groups on the opposite side. Furthermore, another disadvantage of this model is the mismatch between the length of the hydrophobic region of cardiotoxin and that of the lipid core. Finally, according to this model, the central and the C-terminal loops, where most of the β-sheets are located (Rees et al., 1987; Steinmetz et al., 1988) are nearly perpendicular to the bilayer surface, so that more amide C = O groups should be oriented parallel to the bilayer surface, which was not observed from the ATR measurements.

The model of Batenburg et al. (1985) is supported by experimental evidence in the case of cardiolipin. However, this lipid is known to easily adopt nonlamellar structures which is not the case for DMPA. For example, de Kruijff and Cullis (1980) have shown that calcium ions and poly(L-lysine) promote the formation of the inverted hexagonal H_{II} structure in lipid systems containing cardiolipin while complexes of DMPA with calcium or poly(L-lysine) remain lamellar (Laroche et al., 1990, 1991). Therefore, DMPA does not show any ability to adopt the hexagonal H_{II} structure under conditions where cardiolipin does, so that it appears unlikely that this type of structure is the predominant one for the DMPA–cardiotoxin system. This is further supported by the small-angle X-ray diffraction pattern, which is not typical of the hexagonal H_{II} structure (Shyamsunder et al., 1988).

The infrared results presented in this work can be rationalized by the model proposed by Dufourcq et al. (1982). In this model, the toxin stays at the interface due to the presence of tight salt bridges between Lys and Arg residues and phosphate groups, but its N-terminal loop interacts hydrophobically with the acyl chains of DMPA. This wedge effect, favored by the fact that the phosphate group of the lipid is double ionized, is likely at the origin of the conformational disordering of the acyl chains of DMPA. The penetration of the protein into the bilayer is also supported by the increased accessibility of the lipid ester carbonyl groups to the aqueous environment.

The question that arises at this point is what kind of lipid self-assembly is present in the DMPA–cardiotoxin complexes. One possibility is that, in the presence of the protein, the lipids are still packed in lamellae but, according to the small-angle X-ray results, the thickness of the lamellae is fairly variable. Since the order parameters for the amide I, II, and A vibrations are nearly equal to 0 (Table I), the plane of the triple-strand β-sheet formed by the central and C-terminal loops (Steinmetz et al., 1988), which are not embedded into the bilayer, not only is oriented perpendicular to the bilayer surface but must equally lie in the plane of the bilayer. If the N-terminal loop of cardiotoxin is embedded into the DMPA bilayers, the orientation of the toxin molecules is not very homogeneous. Another possibility that accounts for the infrared results is that the structure of DMPA–cardiotoxin complexes is vesicular instead of lamellar. In fact, it has been observed that the formation of double ionized PA leads to the vesiculation of the lipid (Hauser et al., 1990). The existence of such a structure would be at the origin of the poor protein orientation determined from the ATR measurements and of the broad X-ray diffusion patterns.

The results obtained on the effect of cardiotoxin on the equimolar mixture of DMPA and DMPC-d_{54} show that the gel-to-fluid phase transition of both lipids is shifted toward lower temperatures in the presence of the toxin. However, the thermotropic behavior of each phospholipid is quite different in the complexes. In the case of the anionic component, the interaction of cardiotoxin with the lipid mixture decreases both the cooperativity of the phase transition of the lipid and the molecular order of the acyl chains in the gel phase as the proportion of the toxin in the complexes increases. This behavior is similar to that observed for DMPA in DMPA–cardiotoxin complexes and the temperature profiles obtained at $R_i = 5$ for DMPA alone (Figure 2) and for DMPA in the equimolar mixture (Figure 8A) are quite similar. On the other hand, for the zwitterionic component of the lipid mixture, the gel-to-fluid phase transition of the lipid remains cooperative and almost no change is observed in the molecular order of the acyl chains. At $R_i = 5$, the temperature profile of DMPC-d_{54} in the mixture (Figure 8B) is close to that of the pure lipid. This clearly indicates that cardiotoxin induces a partial phase separation in this lipid mixture, one phase containing DMPA-rich domains perturbed by cardiotoxin, while the other phase is composed of regions enriched in DMPC. By assuming that DMPA and DMPC-d_{54} form an ideal mixture in the latter phase, its content of DMPC-d_{54} can be estimated to be about 80% from the observed phase transition temperature. Thus, by the simultaneous and independent determination of both lipid components of a binary mixture, vibrational spectroscopy offers an effective tool for the investigation of phase separation in phospholipid bilayers.

The question that arises from these results is what are the requirements for proteins or polypeptides to induce phase separation in a binary mixture of phospholipids composed of an anionic and a zwitterionic component. To our knowledge, only a few examples exist in the literature showing that basic extrinsic polypeptides or proteins can induce lateral phase separation in binary phospholipid mixtures. Boggs et al. (1977) have shown by differential scanning calorimetry that the myelin basic protein induces phase separation in PG–PC and PA–PC mixtures. It has also been shown by Raman spectroscopy that polylysine of high molecular weight (M_w = 180 000–260 000) produces a partial phase separation in mixtures of DMPA and DMPC (Laroche et al., 1988). Finally, the ability of melittin to induce phase separation in mixtures of DPPG and DSPC has also been demonstrated by Lafleur et al. (1989) using fluorescence and Raman spectroscopy.

All these proteins and peptides have two features in common that could be at the origin of the phase separation phenomenon. First their content of positively charged residues is high. Second, their structure at the lipid interface favors the

maximization of the electrostatic interactions between their positively charged residues and the anionic phospholipid. This particular structure may be either present in the native protein, as in the case of cardiotoxin, or induced upon the interaction of the polypeptide with the lipids as for high molecular weight polylysine (Laroche et al., 1988).

The ability of cardiotoxin to induce phase separation in PA–PC mixtures further supports the model proposed by Dufourcq et al. (1982). In this model, the penetration of the first loop of the protein in the hydrophobic core of the membrane allows efficient electrostatic interactions of the basic residues of the protein that are mainly located in the second loop with the head group of the anionic lipid.

ACKNOWLEDGMENT

The authors are grateful to C.-P. Lafrance for expert technical assistance for X-ray diffraction measurements and to J. Dufourcq for stimulating discussions.

REFERENCES

Asher, I. M., & Levin, I. W. (1977) *Biochim. Biophys. Acta 468*, 63–72.
Babin, Y., D'Amour, J., Pigeon, M., & Pézolet, M. (1987) *Biochim. Biophys. Acta 903*, 78–88.
Batenburg, A. M., Bougis, P. E., Rochat, H., Verkleij, A. J., & de Kruijff, B. (1985) *Biochemistry 24*, 7101–7110.
Blume, A., Hübner, W., & Messner, G. (1988) *Biochemistry 27*, 8239–8249.
Boggs, J. M., Moscarello, M. A., & Papahadjopoulos, D. (1977) *Biochemistry 16*, 5420–5426.
Bougis, P., Rochat, H., Piéroni, G., & Verger, R. (1981) *Biochemistry 20*, 4915–4920.
Bougis, P., Tessier, M., Van Rietschotten, J., Rochat, H., Faucon, J.-F., & Dufourcq, J. (1983) *Mol. Cell. Biochem. 55*, 49–64.
Bougis, P. E., Marchot, P., & Rochat, H. (1986) *Biochemistry 25*, 7235–7243.
Byler, D. M., & Susi, H. (1986) *Biopolymers 25*, 469–487.
Cameron, D. G., Casal, H. L., & Mantsch, H. H. (1980) *Biochemistry 19*, 3665–3672.
Casal, H. L., & Mantsch, H. H. (1984) *Biochim. Biophys. Acta 779*, 381–401.
Casal, H. L., Mantsch, H. H., & Hauser, H. (1987a) *Biochemistry 26*, 4408–4416.
Casal, H. L., Martin, A., Mantsch, H. H., Paltauf, F., & Hauser, H. (1987b) *Biochemistry 26*, 7395–7401.
De Kruijff, B., & Cullis, P. R. (1980) *Biochim. Biophys. Acta 601*, 235–240.
Devlin, M. T., & Levin, I. W. (1989) *Biochemistry 28*, 8912–8920.
Dluhy, R. A., Cameron, D. G., Mantsch, H. H., & Mendelsohn, R. (1983) *Biochemistry 22*, 6318–6325.
Dong, A., Huang, P., & Caughey, W. S. (1990) *Biochemistry 29*, 3303–3308.
Dousseau, F., & Pézolet, M. (1990) *Biochemistry 29*, 8771–8779.
Dousseau, F., Therrien, M., & Pézolet, M. (1989) *Appl. Spectrosc. 43*, 538–542.
Dufourcq, J., & Faucon, J.-F. (1978) *Biochemistry 17*, 1170–1176.
Dufourcq, J., Faucon, J.-F., Bernard, E., Pézolet, M., Tessier, M., Bougis, P., Van Rietschoten, J., Delori, P., & Rochat, H. (1982) *Toxicon 20*, 165–174.
Faucon, J.-F., Dufourcq, J., Bernard, E., Duchesneau, L., & Pézolet, M. (1983) *Biochemistry 22*, 2179–2185.
Fringeli, U. P., & Günthard, H. H. (1981) in *Membrane Spectroscopy*, (Grell, E., Ed.) pp 270–332, Springer-Verlag, New York.
Galla, H. J., & Sackmann, E. (1975) *Biochim. Biophys. Acta 401*, 509–529.
Gennis, R. B. (1989) in *Biomembranes Molecular Structure and Function*, Springer Verlag, New York.
Graham, I., Gagné, J., & Silvius, J. R. (1985) *Biochemistry 24*, 7123–7131.
Griffiths, P. R., & Pariente, G. L. (1986) *Trends Anal. Chem. 5*, 209–215.
Harlos, K., Eibl, H., Pasher, I., & Sundell, S. (1984) *Chem. Phys. Lipids 34*, 115–126.
Hauser, H., Mantsch, H. H., & Casal, H. L. (1990) *Biochemistry 29*, 2321–2329.
Hübner, W., & Mantsch, H. H. (1991) *Biophys. J. 59*, 1261–1272.
Hui, S. W., Boni, L. T., Stewart, T. P., & Isac, T. (1983) *Biochemistry 22*, 3511–3516.
Jacobson, K., & Papahadjopoulos, D. (1975) *Biochemistry 14*, 152–161.
Kouaouci, R., Silvius, J. R., Graham, I., & Pézolet, M. (1985) *Biochemistry 24*, 7132–7140.
Krimm, S., & Bandekar, J. (1986) *Adv. Protein Chem. 38*, 181–364.
Lafleur, M., Faucon, J.-F., Dufourcq, J., & Pézolet, M. (1989) *Biochim. Biophys. Acta 980*, 85–92.
Laroche, G., Carrier, D., & Pézolet, M. (1988) *Biochemistry 27*, 6220–6228.
Laroche, G., Dufourc, E. J., Pézolet, M., & Dufourcq, J. (1990) *Biochemistry 29*, 6460–6465.
Laroche, G., Dufourc, E. J., Dufourcq, J., & Pézolet, M. (1991) *Biochemistry 30*, 3105–3114.
Lauterwein, J., & Wüthrich, K. (1978) *FEBS Lett. 93*, 181–184.
Liao, M.-J., & Prestegard, J. H. (1981) *Biochim. Biophys. Acta 645*, 149–156.
Mendelsohn, R., & Maisano, J. (1978) *Biochim. Biophys. Acta 506*, 192–201.
Mendelsohn, R., & Tarashi, T. (1978) *Biochemistry 17*, 3944–3949.
Ménez, A., Langlet, G., Tamiya, N., & Fromageot, P. (1978) *Biochimie 60*, 505–516.
Ménez, A., Gatineau, E., Roumestand, C., Harvey, A. L., Mouawad, L., Gilquin, B., & Toma, F. (1990) *Biochimie 72*, 575–588.
Muga, A., Surewicz, W. K., Wong, P. T. T., Mantsch, H. H., Singh, V. K., & Shinohara, T. (1990) *Biochemistry 29*, 2925–2930.
Mushayakarara, E., & Levin, I. W., (1984) *Biochim. Biophys. Acta 769*, 585–595.
Onishi, S. I., & Ito, T. (1974) *Biochemistry 13*, 881–887.
Papahadjopoulos, D., Poste, G., & Vail, W. J. (1979) in *Methods in Membrane Biology* (Korn, E. D., Ed.) 10, pp 1–121, Plenum Press, New York.
Pézolet, M., Duchesneau, L., Bougis, P., Faucon, J.-F., & Dufourcq, J. (1982) *Biochim. Biophys. Acta 704*, 515–523.
Pézolet, M., Boulé, B., & Bourque, D. (1983) *Rev. Sci. Instrum. 54*, 1364–1367.
Pézolet, M., Bonenfant, S., Dousseau, F., & Popineau, Y. (1992) *FEBS Lett. 299*, 247–250.
Portis, A., Newton, C., Pangborn, W., & Papahadjopoulos, D. (1979) *Biochemistry 18*, 780–790.
Poste, G., & Allison, A. C. (1973) *Biochim. Biophys. Acta 300*, 421–465.
Rivas, E. A., Le Maire, M., & Gulik-Krzywicki, T. (1981) *Biochem. Biophys. Acta 644*, 127–133.
Rothschild, K., & Clark, N. A. (1979) *Biophys. J. 25*, 473–478.
Rees, B., Samama, J. P., Thierry, J. C., Gilibert, M., Fischer, J., Schweitz, H., Lazdunski, M., & Moras, D. (1987) *Proc. Natl. Acad. Sci. U.S.A. 84*, 3132–3136.
Sackmann, E. (1983) in *Biophysics* (Hoppe, W., Lohmann, W., Markl, H., & Ziegler, H., Eds.) pp 425–457, Springer-Verlag, Berlin.
Scheule, R. K. (1987) *Biochim. Biophys. Acta 889*, 185–195.
Shimanouchi, T., Tsuboi, M., & Kyogoku, Y. (1964) *Adv. Chem. Phys. 7*, 435–498.

Shyamsunder, E., Gruner, S. M., Tate, M. W., Turner, D. C., So, P. T. C., & Tilcock, C. P. S. (1988) *Biochemistry 27*, 2332–2336.

Snyder, R. G., Hsu, S. L., & Krimm, S. (1978) *Spectrochim. Acta 34A*, 395–406.

Steinmetz, W. E., Bougis, P. E., Rochat, H., Redwine, O. D., Braun, W., & Wüthrich, K. (1988) *Eur. J. Biochem. 172*, 101–116.

Sunder, S., Cameron, D., Mantsch, H. H., & Bernstein, H. J. (1978) *Can. J. Chem. 56*, 2121–2126.

Surewicz, W. K., & Mantsch, H. H. (1988) *Biochim. Biophys. Acta 952*, 115–130.

Surewicz, W. K., Stepanik, T. M., Szabo, A. G., & Mantsch, H. H. (1988) *J. Biol. Chem. 263*, 786–790.

Surewicz, W. K., Leddy, J. J., & Mantsch, H. H. (1990) *Biochemistry 29*, 8106–8111.

Thomas, L. C., & Chittenden, R. A. (1964) *Spectrochim. Acta 20*, 489–502.

Thomas, L. C., & Chittenden, R. A. (1970) *Spectrochim. Acta 26*, 781–800.

Traüble, H., & Eibl, H. (1974) *Proc. Natl. Acad. Sci. U.S.A. 71*, 214–219.

Umemura, J., Cameron, D. G., & Mantsch, H. H. (1980) *Biochim. Biophys. Acta 602*, 32–34.

Van Dijck, P. W. M., de Kruijff, B., Verkleij, A. J., Van Deenen, L. L. M., & de Gier, J. (1978) *Biochim. Biophys. Acta 512*, 84–96.

Vincent, J. P., Balerna, M., & Lazdunski, M. (1978) *FEBS Lett. 85*, 103–108.

Visser, L., & Louw, A. I. (1978) *Biochim. Biophys. Acta 533*, 80–89.

Registry No. DMPA, 28874-52-4; DMPC, 18194-24-6.